POLITECNICO

MILANO 1863

Flight trajectory optimization of Ground-Gen airborne wind energy systems through a harmonic balance method

TESI DI LAUREA MAGISTRALE IN
AEROSPACE ENGINEERING - INGEGNERIA AEROSPAZIALE

Author: **Aitor Doménech Moreno**

Student ID: 219786
Advisors: Filippo Trevisi and Alessandro Croce
Academic Year: 2022-23

Abstract

In the following thesis the study of the optimal control problem for flight trajectories of Ground-Gen airborne wind energy system (AWES) is achieved, being one of the novelties of the present work the expression of the optimal control problem in the frequency domain through a harmonic balance formulation.

Firstly, an introduction to Airborne Wind Energy (AWE) is done describing the different types of airborne units, also, the steady-state model is presented. Then, the flight dynamic model is introduced with its corresponding equations and reference frames. Assuming that the reel-out velocity is only considered in the aerodynamic forces, not included then in the inertial forces term. Afterwards, the frequency domain formulation description is presented, where the trajectory is described by the Fourier coefficients of the dynamics (elevation and azimuth angles) and of the control inputs (AWES roll angle and gamma, which refers to the ratio between the reel-out velocity and the wind speed). Then, the optimal control problem approach is described.

Furthermore, the conclusions of the thesis are stated from the results of the optimal control problem, when considering idealized cases with uniform incoming wind speed and no constraints in the minimum elevation angle. If gravity is neglected, the solution is steady, and it can be described by analytical expressions. On the other hand, if gravity is considered, the solutions are no more constant. If the aim is to maximize the mean mechanical power considering it as the objective function, the ideal trajectories for Ground-Gen AWES are circular in shape, maintaining a constant AWES velocity and with the wing span perpendicular to the incoming wind. Also, optimal solutions present negative mean elevation angle.

Keywords: Airborne Wind Energy System, Ground-Gen, harmonic balance method, frequency domain formulation, trajectory optimization

Contents

Introduction

Airborne Wind Energy (AWE) makes reference to the branch of wind energy which focus on harvesting power from the wind by means of airborne systems. Making the comparison with traditional wind turbines, it can be found two main advantages for Airborne Wind Energy Systems (AWESs). On the one hand, at higher altitudes there is access to better wind resource availability. And on the other hand, AWESs reduce in a significant way the mass for the same power output, therefore reducing production costs. Furthermore, AWESs can be classified regarding to flight operations, which are connected to the way of generating power. The different flight operations which can be considered are crosswind, tether-aligned and rotational. However, current research on the topic technology marks that most companies and institutes are centering on AWESs which generate aerodynamic lift by flying crosswind [1, 2].

In addition, AWESs can be mainly divided in two categories depending on how the electrical power is generated. As power can be generated with an electric generator placed on a fixed or a moving ground station, or, alternatively, by means of on-board wind turbines. In the first case the system, so called Ground-Gen AWES, is characterized for producing power in cycles. In the power production cycle, power is produced by the kite pulling and unwinding a tether from a drum connected to the generator. In the rewinding cycle, a part of the produced energy is used to wind the kite back to the starting position in a low traction mode. In the second generation type the system, so called Fly-Gen AWES, produces power by means of on-board wind turbines and transmits it to the ground using electric cables embedded in the tether. The wing type, soft or fixed, additionally classifies the AWESs. Nowadays, no category has clear advantages with respect to the other one and companies and research institutions are developing both concepts [2, 3]. Figure 1 shows a graphical comparison of both AWESs.
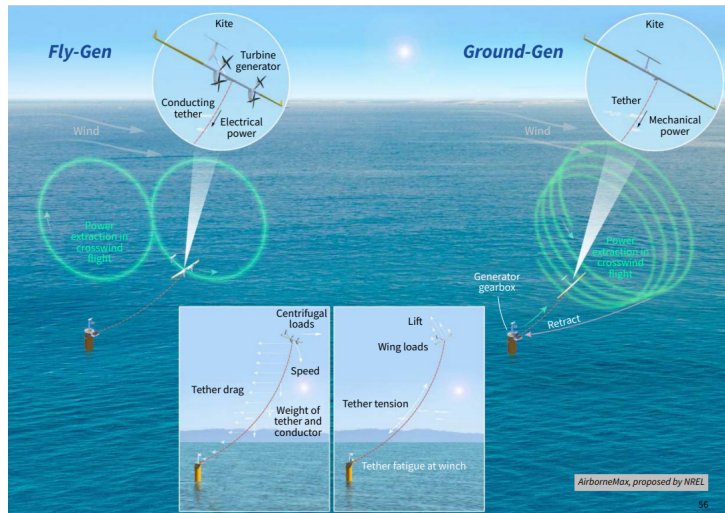
Figure 1: Comparison between Ground-Gen and Fly-Gen AWES [1].

Although the existence of these two categories, this thesis focuses on AWESs based on fixed-wing with ground station generation, known as Ground-Gen AWESs. Therefore, the main aim of this thesis is to rework on the dynamic model used for Fly-Gen [3] by establishing new dynamic equations appropriate for Ground-Gen instead.

The methods selected in the thesis allow to investigate optimal trajectories of AWESs for a better knowledge of their physical characteristics. Setting then another goal of the thesis, the interpretation of the physical characteristics of optimal trajectories and the analysis of how they are influenced by parameters describing the system and its operation. By doing this, solutions might be compared with analytical results from first-principle models. Then, for achieving this goal a low-fidelity dynamic model, similar to the one proposed by Fernandes [4] (reformulated for Ground-Gen AWESs), is chosen. Rather than solving the dynamics and the optimal control problem in time, the present approach models the problem in the frequency domain, making use of a harmonic balance method, which expands the periodic solution as a Fourier series. By working with Fourier coefficients instead of time series allows a significant reduction of the problem size depending on the problem at hand, searching for periodic solutions implicitly and the study of the solution in an intuitive way by looking at the contribution of the different harmonics.

The paper is organised as follows: in Chapter 1 firstly the steady-state model is presented together with the introduction of some key non-dimensional numbers used later in the analyses. Also, the flight dynamic model, the frequency-domain formulation and the optimal control problem are introduced afterwards. In Chapter 2 optimal control problem results with constant wind inflow and no constraints on the mean elevation angle are

analyzed. Including the optimization for the mean electrical power in the absence of gravity and the optimization of the mean mechanical power considering gravity. Finally, in Chapter 3 the results are discussed and the main conclusions summarized.

1 | Methodology

1.1. Steady-state model

In this section a simplified and idealized derivation of the power equation regarding Ground-Gen AWES is explained, in order to present and understand both, the physics and the terminology which are employed in later sections of the thesis. It is remarkable that the derivation focuses only on the production phase power, which is when the kite is pulling and unwinding the tether, not modeling then the recovery phase. Firstly, the assumptions considered are the following ones:

- Consideration of equilibrium of the external forces acting on the kite, being the inertial forces null. Neglecting mass, trajectory of the kite and gravity.

- Constant wind speed is aligned with the tether length direction, as it is not considered an elevation angle of the tether yet.

- Straight positioning of the tether. Adequate assumption for small tether sag as its effects can be considered with alternative models in the power equation.
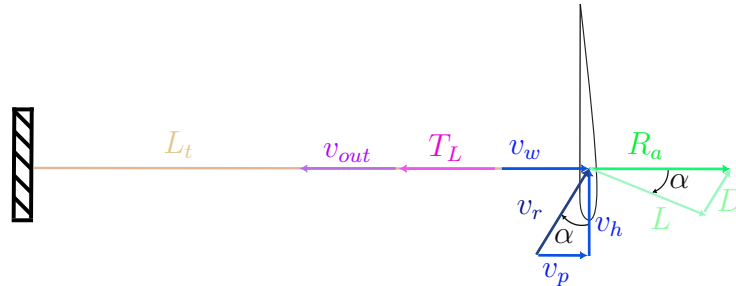

Figure 1.1: Velocity triangle and aerodynamic forces for Ground-Gen AWES.

Considering Fig. 1.1, L corresponds to the lift of the kite, D its drag and by the combination of these two aerodynamic forces R_a is obtained, defined as the resultant aerodynamic

force. Then, T_L corresponds to the tether force and v_{out} is the reel-out velocity of the tether. Furthermore, the perpendicular velocity to the kite is introduced as $v_p = v_w - v_{out}$, being v_w the wind speed itself. Therefore, the ideal power for Ground-Gen corresponds to the tether force multiplied by the reel-out velocity:

$$P_{m,L} = T_L \cdot v_{out} \tag{1.1}$$

Under the assumption of steady-state flight, it is considered that R_a is parallel to the the tether and D has the same direction as the relative velocity v_r. Then, by means of trigonometric relations with respect to the angle of attack α, and assuming its value as a small one, $\alpha \ll 1$, the following relation can be obtained:

$$\alpha \approx \frac{D}{L} = \frac{\frac{1}{2}\rho A C_D v_r^2}{\frac{1}{2}\rho A C_L v_r^2} = \frac{1}{G} \approx \frac{v_p}{v_h} \tag{1.2}$$

Being G the glide ratio, defined as $\frac{C_L}{C_D}$, and v_h being the horizontal component of the relative velocity of the kite parallel to the chord. Then, a simplified expression for v_r can be obtained, by introducing the parameter $\gamma_{out} = \frac{v_{out}}{v_w}$. Furthermore, considering that the tether force is equal to the resultant aerodynamic force, T_L can be defined as:

$$\begin{cases} v_r^2 = v_p^2 + v_h^2 = v_p^2 \cdot (1 + G^2) = v_w^2 \cdot (1 - \gamma_{out})^2 \cdot (1 + G^2) \\ T_L^2 = R_a^2 = L^2 + D^2 = L^2 \cdot (1 + \dfrac{1}{G^2}) \\ T_L = \dfrac{1}{2}\rho A \cdot v_w^2 \cdot (1 - \gamma_{out})^2 \cdot \dfrac{C_L}{G} \cdot (1 + G^2)^{\frac{3}{2}} \end{cases} \tag{1.3}$$

Also, the previous equation can be simplified by assuming high values for the glide ratio, $G^2 \gg 1$, obtaining:

$$\begin{cases} v_r^2 \approx v_w^2 \cdot (1 - \gamma_{out})^2 \cdot G^2 \\ T_L \approx \dfrac{1}{2}\rho A \cdot v_w^2 \cdot (1 - \gamma_{out})^2 \cdot C_L \cdot G^2 \end{cases} \tag{1.4}$$

Then by substituting T_L from Eq. (1.3) into Eq. (1.1) the ideal mechanical power equation results in:

$$P_{m,L} = T_L \cdot v_{out} = \frac{1}{2}\rho A \cdot v_{out} \cdot v_w^2 \cdot (1 - \gamma_{out})^2 \cdot \frac{C_L}{G} \cdot (1 + G^2)^{\frac{3}{2}} \tag{1.5}$$

Once, defined the power equation, for finding out the maximum power it can be taken

the derivative of $P_{m,L}$ with respect to v_{out}, being the maximum power when $v_{out} = \frac{v_w}{3}$:

$$P_{m,L,max} = \frac{2}{27}\rho A \cdot v_w^3 \cdot \frac{C_L}{G} \cdot (1 + G^2)^{\frac{3}{2}} \tag{1.6}$$

In addition, if it is considered the generator and transmission efficiency, η_{el}, the ideal electrical power generated can be obtained, by just multiplying the mentioned efficiency with the ideal mechanical power from Eq. (1.5):

$$P_L = \eta_{el} \cdot P_{m,L} \tag{1.7}$$

Secondly, for advancing with the steady-state model formulation, new considerations are taken into account [5]. For performing a simple equilibrium of forces of the model, now mass and the radius of the trajectory of the kite are considered. Then, centrifugal force appears as an external force, as seen in Fig. 1.2. Also, new parameters are considered such as R_o which marks the radius of the trajectory of the kite and Φ, the opening angle, which denotes the angle swept by the AWES during the circular trajectory. In addition, the ground reference system (denoted by $\mathcal{F}_G$) is defined, being inertial and centered at the ground station. Having $\boldsymbol{e_x}$ pointing downwind, $\boldsymbol{e_y}$ pointing in the centrifugal direction of the trajectory and $\boldsymbol{e_z}$ completes the right-handed frame.
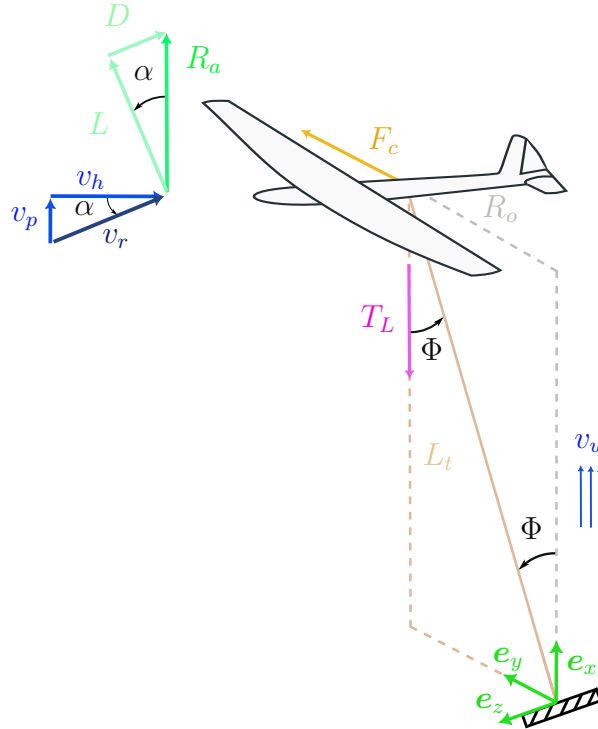

Figure 1.2: Centrifugal force of the kite and 3D representation of steady-state model.

Focusing on Fig. 1.2 a relation of forces can be reached by assuming $\alpha \ll 1$, or what is the same $G^2 \gg 1$, and relating aerodynamic forces with centrifugal ones:

$$\begin{cases} L \approx R_a = \dfrac{1}{2}\rho A \cdot C_L \cdot v_r{}^2 \\ R_a \tan \Phi = F_c = m\dfrac{v_h^2}{R_o} \rightarrow \sin \Phi \tan \Phi = M \cdot \dfrac{v_h^2}{v_r^2} = M \cdot \dfrac{1}{1 + \frac{1}{G^2}} \end{cases} \tag{1.8}$$

Again, if a high glide ratio is considered, $G^2 \gg 1$ the previous equation could be simplified by taking $\frac{v_h^2}{v_r^2} \approx 1$. Being, M defined as the non-dimensional mass parameter, and m the mass of the kite itself:

$$M = \frac{m}{\frac{1}{2}\rho A \cdot C_L \cdot L_t} \tag{1.9}$$

Also in this idealized case, the turning radius is $R_o = L_t \sin \Phi$ and the revolution period is defined as:

$$\mathcal{T}_L = \frac{2\pi R_o}{v_L} = \frac{2\pi R_o}{v_p G} \tag{1.10}$$

where v_L is the norm of the AWES velocity. In addition to the non-dimensional mass parameter, the Froude number, which weights the fluid inertial forces to gravity forces, is used in this thesis:

$$F_r = \sqrt{\frac{v_w^2}{g \cdot L_t}} \tag{1.11}$$

where the reference velocity is the wind velocity and the reference length is the tether length. By combining the previously introduced non-dimensional parameters, the gravity ratio G_r is defined as the ratio between gravitational force and aerodynamic lift:

$$G_r = \frac{M}{F_r^2 G^2 (1 - \gamma_{out})^2} = \frac{mg}{\frac{1}{2}\rho A C_L v_w^2 G^2 (1 - \gamma_{out})^2} \tag{1.12}$$

m	2000 kg	A	54 m²	γ	1/3	v_L	48 m s⁻¹	C_D	0.15
η_{el}	0.9	ρ	1.225 kg m⁻³	g	9.81 m s⁻²	v_w	6 m s⁻¹	C_L	1.8
G	12	M	0.1120	$\mathcal{T}_L$	12.74 s	Fr	0.1106	G_r	0.1430
L_t	300 m	T_L	138.60 kN	$P_{m,L}$	277.20 kW	P_L	249.48 kW		

Table 1.1: Reference values for the examples (values from Makani MX2), associated non-dimensional parameters and quantities evaluated with the steady-state model for maximizing Eq. (1.7).

Finally, as an ending for this section, it is remarkable to say that these idealized analytical

expressions will permit the comparison and validation of results of the optimal control problem formulation for next sections of the thesis. Also, input parameters from Makani MX2 [6] design will be used as reference values to present the results as seen in Table 1.1. Although Makani MX2 is a Fly-Gen AWES, this inputs have been considered just as reference in order to get a physical understanding of the model.

1.2.   Flight dynamic model

Once the steady-state model with its idealized power equations has been explained, the next section focuses on the flight dynamic model for the analysed Ground-Gen AWES. Therefore, this section comprises the deep explanation of the dynamic model itself together with its own characteristics and reference frames. Adding that the problem of study is not fully periodic, but it is desired be periodic in order that some assumptions can be considered on the model.

The flight dynamic model not includes the reel-out velocity in the dynamics, this velocity is just taken into consideration in the aerodynamic forces. Furthermore, it is based in two coordinate systems as seen in Fig. 1.3 (a). The ground coordinate system, denoted as $\mathcal{F}_G$, which is the same employed before for the explanation of the steady-state model, being inertial and centered at the ground station: $\boldsymbol{e_x}$ points downwind, $\boldsymbol{e_z}$ toward the Zenith and $\boldsymbol{e_y}$ completes the right-handed frame. For convenience, in order to describe the position of the airborne unit spherical coordinates are employed, being L_t the tether length, ϕ the azimuth angle and β the elevation angle. The second spherical reference frame, $\mathcal{F}_S$, is defined at every position with the origin at the AWES center of mass. Containing, $\boldsymbol{e_r}$ pointing outward the sphere in the radial direction, $\boldsymbol{e_\phi}$ normal to $\boldsymbol{e_r}$ and contained on a plane parallel to $x - y$ and $\boldsymbol{e_\beta} = \boldsymbol{e_r} \times \boldsymbol{e_\phi}$. The three vectors defining the $\mathcal{F}_S$ reference system can be defined in terms of the ground reference system components in the following way:

$$\begin{cases} \boldsymbol{e_r} = (\cos\phi\cos\beta)\boldsymbol{e_x} + (\cos\beta\sin\phi)\boldsymbol{e_y} + (\sin\beta)\boldsymbol{e_z} \\ \boldsymbol{e_\phi} = -(\sin\phi)\boldsymbol{e_x} + (\cos\phi)\boldsymbol{e_y} \\ \boldsymbol{e_\beta} = -(\cos\phi\sin\beta)\boldsymbol{e_x} - (\sin\beta\sin\phi)\boldsymbol{e_y} + (\cos\beta)\boldsymbol{e_z} \end{cases} \tag{1.13}$$

Once defined $\boldsymbol{e_r}$, $\boldsymbol{e_\phi}$ and $\boldsymbol{e_\beta}$, the position $\boldsymbol{p}$, velocity $\boldsymbol{v}$ and acceleration $\boldsymbol{a}$ of the airborne

unit projected into the spherical reference frame $\mathcal{F}_S$ are determined:

$$
\begin{cases}
\boldsymbol{p} = L_t \boldsymbol{e}_r \\
\boldsymbol{v} = L_t \dot{\phi} \cos \beta \boldsymbol{e}_\phi + L_t \dot{\beta} \boldsymbol{e}_\beta \\
\boldsymbol{a} = \left(-L_t \dot{\phi}^2 \cos^2 \beta - L_t \dot{\beta}^2 \right) \boldsymbol{e}_r + \left(L_t \ddot{\phi} \cos \beta - 2 L_t \dot{\phi} \dot{\beta} \sin \beta \right) \boldsymbol{e}_\phi \\
\quad + \left(L_t \dot{\phi}^2 \sin \beta \cos \beta + L_t \ddot{\beta} \right) \boldsymbol{e}_\beta
\end{cases}
\tag{1.14}
$$

Furthermore, the wind velocity is in the positive x-axis direction of $\mathcal{F}_G$ and projected into the spherical reference frame is:

$$
\begin{cases}
\boldsymbol{v}_w = v_w \left(\cos \phi \cos \beta \boldsymbol{e}_r - \sin \phi \boldsymbol{e}_\phi - \cos \phi \sin \beta \boldsymbol{e}_\beta \right) \\
v_w(h) = v_{w,0} \left(\dfrac{h}{h_0} \right)^{\alpha_s} = v_{w,0} \left(\dfrac{L_t}{h_0} \sin \beta \right)^{\alpha_s}
\end{cases}
\tag{1.15}
$$

where the wind speed v_w as function of the altitude h is modelled with an exponential law: $v_{w,0}$ is the reference wind speed at the reference altitude h_0 and α_s is the wind shear exponent.

The defined dynamic model sets that the reel-out velocity, $\boldsymbol{v}_{out}$, is linked with $\dot{L}_t$, although in reality it is not exactly just $\dot{L}_t$, as there are trigonometric relations in between both variables. In addition, $\boldsymbol{v}_{out}$ is only considered in the lift and drag aerodynamic forces terms. Not considering then, the effects of $\dot{L}_t$ and $\ddot{L}_t$ in $\boldsymbol{v}$ and $\boldsymbol{a}$, and therefore not included in the inertial forces term. With this assumption, the relative speed between the AWES and the wind is:

$$
\boldsymbol{v}_r = \boldsymbol{v}_w - (\boldsymbol{v} + \boldsymbol{v}_{out})
\tag{1.16}
$$

For describing the AWES attitude, a non-sideslip velocity constraint is included in the modeling. Indeed, the wing operates at the highest performance under this condition. To impose this constraint implicitly, the unit vector $\boldsymbol{e_1}$ is defined to point the opposite direction of the relative wind speed:

$$
\boldsymbol{e}_1 = -\frac{\boldsymbol{v}_r}{|\boldsymbol{v}_r|}
\tag{1.17}
$$

The span wise unit vector $\boldsymbol{s}$ (with origin at the center of mass and pointing in the right-wing span direction) is defined perpendicular to $\boldsymbol{e_1}$ with the procedure illustrated in Fig. 1.3 (b). A second vector $\boldsymbol{e_3}$ is defined as a unit vector in a plane parallel to the $x - z$
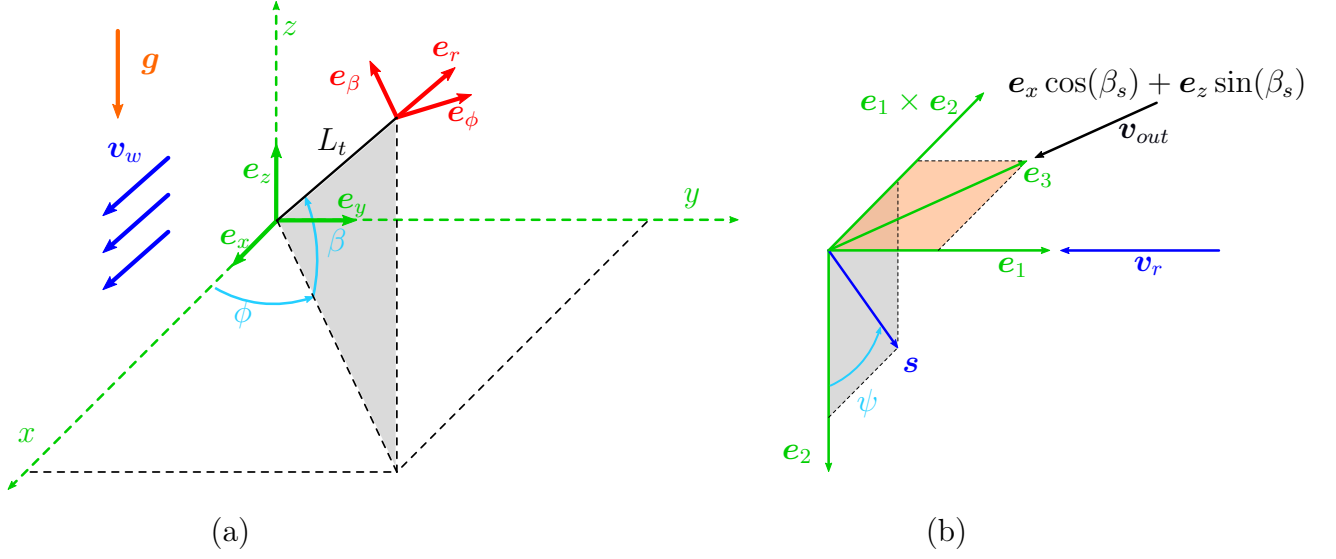
(a)

(b)

Figure 1.3: **(a)** Ground reference frame $\mathcal{F}_G$ ($\mathbf{e}_x - \mathbf{e}_y - \mathbf{e}_z$) and spherical reference frame $\mathcal{F}_S$ ($\mathbf{e}_r - \mathbf{e}_\phi - \mathbf{e}_\beta$) and **(b)** sketch for the spanwise unit vector $\mathbf{s}$ definition.

plane with elevation β_s (and negative sign):

$$
\begin{cases}
\boldsymbol{e}_3 = -(\boldsymbol{e}_x \cos(\beta_s) + \boldsymbol{e}_z \sin(\beta_s)) \\
\boldsymbol{e}_x = (\cos\phi\cos\beta)\boldsymbol{e}_r - (\sin\phi)\boldsymbol{e}_\phi - (\cos\phi\sin\beta)\boldsymbol{e}_\beta \\
\boldsymbol{e}_z = (\sin\beta)\boldsymbol{e}_r + (\cos\beta)\boldsymbol{e}_\beta
\end{cases}
\tag{1.18}
$$

Note that $\boldsymbol{e_3}$ points upwind when $\beta_s = 0$. The unit vector $\boldsymbol{e_2}$ is then defined as:

$$
\boldsymbol{e}_2 = \frac{\boldsymbol{e}_3 \times \boldsymbol{e}_1}{|\boldsymbol{e}_3 \times \boldsymbol{e}_1|}
\tag{1.19}
$$

where $|\boldsymbol{e}_3 \times \boldsymbol{e}_1|$ can take values smaller than one because $\boldsymbol{e_3}$ and $\boldsymbol{e_1}$ are not defined to be perpendicular in general. In this way, $\boldsymbol{e_2}$ is perpendicular to the plane $\boldsymbol{e_3}$-$\boldsymbol{e_1}$. Rodrigues' formula is then used to define $\boldsymbol{s}$ through a rotation of ψ around $\boldsymbol{e_1}$, starting from $\boldsymbol{e_2}$:

$$
\boldsymbol{s} = \boldsymbol{e}_2 \cos\psi + (\boldsymbol{e}_1 \times \boldsymbol{e}_2)\sin\psi + \boldsymbol{e}_1 (\boldsymbol{e}_1 \cdot \boldsymbol{e}_2)(1 - \cos\psi)
\tag{1.20}
$$

With this formulation, $\boldsymbol{s}$ is defined to be always perpendicular to the relative wind and its components are defined by a unique angle ψ, called hereafter roll angle. When $\psi = 0$,

s is perpendicular to e_3. The aerodynamic lift L and the drag D take the standard form:

$$\begin{cases} L = \dfrac{1}{2}\rho A C_L \left|v_r\right| v_r \times s \\ D = \dfrac{1}{2}\rho A C_D \left|v_r\right| v_r \end{cases} \tag{1.21}$$

where ρ is the air density, A is the wing area and the lift and drag coefficients C_L and C_D are considered constant. The drag coefficient C_D includes the contribution from the tether drag. The gravitational force F_g and the tether force T are:

$$\begin{cases} F_g = -mg(\sin\beta e_r + \cos\beta e_\beta) \\ T = -T e_r \end{cases} \tag{1.22}$$

where m is the AWES mass, g the gravitational acceleration and T the norm of the tether force. The dynamic equations of motion in compact are:

$$ma = L + D + F_g + T \tag{1.23}$$

recalling that a is given by Eq. (1.14). In the flight dynamic model γ is defined then as:

$$\gamma = \frac{v_{out}}{v_w} \tag{1.24}$$

As the objective of optimal control problem is related to power production, as done in the steady-state model, two power quantities are going to be defined, the mechanical power P_m and the electrical power of the model P. Then, P_m is defined as the scalar product of the tether force and the reel-out velocity:

$$P_m = -T \cdot v_{out} \tag{1.25}$$

And the electrical power is obtained by considering the generator and transmission efficiency, η_{el}, in the following way:

$$P = \begin{cases} P_m - (1 - \eta_{el})P_m & \text{for} \quad \gamma \geq 0 \\ P_m + (1 - \eta_{el})P_m & \text{for} \quad \gamma < 0 \end{cases} \tag{1.26}$$

When power is generated ($\gamma > 0$), the electrical power distributed to the grid P is lower than the mechanical power P_m because of electrical efficiencies. When power from the grid is used, the electrical power requested to the grid P is instead higher in absolute value compared to the mechanical power P_m. To model the discontinuity in a continuous

optimization framework, the logistic function is used:

$$P = P_m - \left(\frac{1 - e^{-f\gamma}}{1 + e^{-f\gamma}}\right)(1 - \eta_{el})P_m \qquad (1.27)$$

where f is taken equal to 100.

1.3. Frequency-domain formulation

In this section the description of the implementation of the frequency-domain formulation is achieved. Frequency-domain formulations might be advantageous when solving for periodic solutions of dynamic and control problems. They are capable of solving in an efficient way for both stable and unstable branches of periodic solutions. In addition, they make use of less variables for describing the same problems. As the problem of optimizing trajectories for AWESs has a periodic nature, the previous flight dynamic model is expressed in the frequency domain. Then, the function of the harmonic balance method is to transform the differential equations of motion into a set of nonlinear algebraic equations [7]. So, the equations of motion (Eq. 1.23) of the flight dynamic model can be written as a set of second order nonlinear differential equations, with the same procedure as for Fly-Gen AWES [3], in the form:

$$\boldsymbol{f}(\mathbf{x}, \dot{\mathbf{x}}, \ddot{\mathbf{x}}, \mathbf{u}) = \mathbf{0} \qquad \mathbf{x} = \begin{bmatrix} \beta(t), \ \phi(t) \end{bmatrix}^T \qquad \mathbf{u} = \begin{bmatrix} \psi(t), \ \gamma(t) \end{bmatrix}^T \qquad (1.28)$$

where $\mathbf{x}$ is the state vector and $\mathbf{u}$ is the control vector. By assuming that Eq. (1.28) accepts periodic solutions, every variable of the state vector is expanded as a Fourier series of order $\boldsymbol{N_x}$:

$$\begin{cases} x(t) \approx \dfrac{X_0}{2} + \displaystyle\sum_{k=1}^{N_x} X_{k,s} \sin\left(k\omega t\right) + X_{k,c} \cos\left(k\omega t\right) \\ \mathbf{X} = \begin{bmatrix} X_0, \ X_{1,s}, \ X_{2,s}, \ ...X_{1,c}, \ X_{2,c}, \ ... \end{bmatrix}^T \end{cases} \qquad (1.29)$$

with $\omega = \dfrac{2\pi}{\mathcal{T}}$ being the fundamental frequency of the motion and $\mathcal{T}$ the period. Then, the first and second derivatives of the state vector can be determined analytically. In addition, the control inputs are also assumed as periodic and are expressed in terms of a

Fourier series of order N_u:

$$
\begin{cases}
u(t) \approx \dfrac{U_0}{2} + \displaystyle\sum_{k=1}^{N_u} U_{k,s} \sin\left(k\omega t\right) + U_{k,c} \cos\left(k\omega t\right) \\[2mm]
\mathbf{U} = \left[U_0, \ U_{1,s}, \ U_{2,s}, \ ...U_{1,c}, \ U_{2,c}, \ ... \right]^T
\end{cases}
\tag{1.30}
$$

where $N_u < N_x$ because the equations of motion need to be solved at frequencies higher than the control inputs order. By replacing Eq. (1.29) and (1.30) together with the analytical second derivative of the state vector into Eq. (1.28), the equations of motion can be expanded as a Fourier series of order N_x:

$$
\begin{cases}
\mathbf{f}(\mathbf{X}_\beta, \mathbf{X}_\phi, \mathbf{U}_\psi, \mathbf{U}_\gamma, \omega, t) \approx \dfrac{\mathbf{F}_0}{2} + \displaystyle\sum_{k=1}^{N_x} \mathbf{F}_{k,s} \sin\left(k\omega t\right) + \mathbf{F}_{k,c} \cos\left(k\omega t\right) = \mathbf{0} \\[2mm]
\mathbf{F} = \left[\mathbf{F}_0, \ \mathbf{F}_{1,s}, \ \mathbf{F}_{2,s}, \ ...\mathbf{F}_{1,c}, \ \mathbf{F}_{2,c}, \ ... \right] = \mathbf{0}
\end{cases}
\tag{1.31}
$$

For given periodic control inputs and a given fundamental frequency, the periodic solution can be found by looking for the Fourier coefficients $[\mathbf{X}_\beta; \mathbf{X}_\phi]$. Furthermore, more detailed formulation and explanation of this section is found in the Fly-Gen AWES document [3].

1.4.   Optimal control problem (OCP)

In this thesis, an optimal control problem (OCP) is included in the frequency domain formulation, again as done for Fly-Gen AWES [3]. A generic optimization problem can be written as:

$$
\begin{aligned}
\mathcal{X}^* \ \ &= \arg\left(\min_{\mathcal{X}} \ obj(\mathcal{X})\right) \\
\text{s.t.:} \ \ &\mathbf{lb} \leq \mathcal{X} \leq \mathbf{ub} \\
&\mathbf{g}(\mathcal{X}) \leq 0 \\
&\mathbf{h}(\mathcal{X}) = 0
\end{aligned}
\tag{1.32}
$$

where $\mathcal{X}$ are the unknown optimization variables, $\mathcal{X}^*$ their optimal values, obj the objective function, $\mathbf{lb}$ and $\mathbf{ub}$ the lower and upper bounds of $\mathcal{X}$, $\mathbf{g}$ the inequality and $\mathbf{h}$ the equality constraints. In the present formulation, the optimization variables are the Fourier coefficients of the state variables, of the control inputs and the fundamental frequency:

$$
\mathcal{X} = [\mathbf{X}_\beta; \mathbf{X}_\phi; \mathbf{U}_\psi; \mathbf{U}_\gamma; \omega]
\tag{1.33}
$$

The negative value of the mean mechanical power $\hat{P}_m$ (Eq. 1.25) or electrical power $\hat{P}$ (Eq. 1.27) over the loop is taken as objective function, where the symbol $\char`\^{}$ stands for the

mean value over the loop. The equality constraints are the aggregation of the residuals of the equation of motion in the frequency domain $\mathbf{F}$ (Eq. 1.31) and additional physical constraints $\mathbf{R}$ in the frequency domain (e.g. certain quantities can be imposed to be constant over the loop):

$$\mathbf{h}(\mathcal{X}) = [\mathbf{F}(\mathcal{X}); \mathbf{R}(\mathcal{X})] = \mathbf{0} \tag{1.34}$$

Inequality constraints $\mathbf{g}$, expressed in the time domain, can also be included in the problem (e.g. the minimum elevation angle over the loop can be bounded). A graphical representation of the OCP setup is given in Fig. 1.4. The derivatives of flight dynamic model with respect to the optimization variables can be taken analytically and provided to the solver, allowing for a deep and fast convergence of the solution. The OCP is implemented in *MATLAB*® environment and solved with the interior-point algorithm implemented in *fmincon*. As the chosen optimization algorithm (gradient-based) can only look for local optima, the initial guess may influence the solution. In this work, the initial guesses are taken to be circular trajectories, leading to circular shaped optimal trajectories. Again, more detailed formulation and explanation of this section is found in the Fly-Gen AWES document [3].
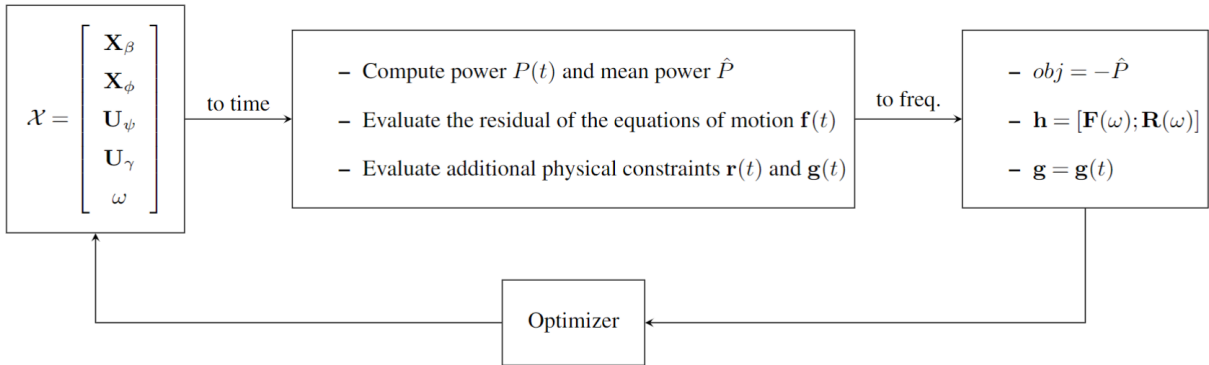

Figure 1.4: Graphical representation of the optimal control problem setup.

2 | Optimal control problem results

Given that the analysis focuses on circular paths, a cylindrical frame of reference called $\mathcal{F}_C$ is employed, same as the framework stated in the previous Fly-Gen work [3]. Figure 2.1 provides a visual depiction of $\mathcal{F}_C$. The longitudinal axis of $\mathcal{F}_C$ aligns with the mean elevation angle $\hat{\beta}$. The angles β_m and Φ represent the minimum elevation angle and the opening angle, respectively. The angular position of the AWES is determined by α , and when $\alpha = 0$, the AWES ascends (i.e., $\dot{\alpha} > 0$).

To gradually introduce increasing complexity, the optimal control problems (OCPs) are adjusted from an idealized scenario to a more realistic one. The idealized cases analyzed in this section assume a uniform incoming wind speed ($\alpha_s = 0$) and impose no constraints on the minimum elevation angle. In this section, β_s (Eq. 1.18) is set to zero, causing $\boldsymbol{e}_3$ to point upwind. Consequently, when the roll is zero ($\psi = 0$), the span direction becomes perpendicular to the incoming wind.
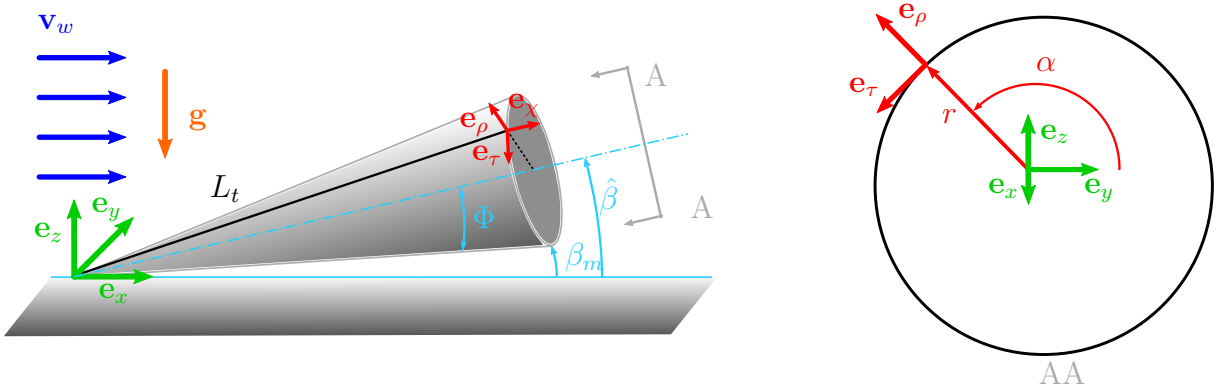

Figure 2.1: Cylindrical reference system $\mathcal{F}_C$ used to analyze circular trajectories.

2.1. Optimizing for the mean electrical power in the absence of gravity

In the most ideal scenario, when gravity is negligible (g = 0), it results that $F_r \to \infty$ and $G_r = 0$. The objective function is defined as the average electrical power in Eq. (1.27). Solving the OCP for the example given in Table 1.1 reveals that the solution remains constant throughout the trajectory, and the average power output matches the value obtained using the analytical expression from Eq. (1.7). Figure 2.2 illustrates the evolution of β and α, clearly indicating that the solution forms a circular path. With the solution's constant values, various quantities such as tether force along the axial symmetry axis, AWES velocity, and others can be determined using the formulation explained in Sect. 1.1.

In order for the solution to be optimal, it has been found that the AWES span should be perpendicular to the direction of the wind speed. This can also be expressed analytically as the parameter $\psi = 0$. Figure 2.2 displays the optimal opening angle Φ^* as a function of a modified non-dimensional mass parameter M_t, derived from solving multiple OCPs with different G ($G \in [6.5 \ 42]$) and M ($M \in [0.03 \ 0.2]$). The values of Φ^* can be accurately described by:

$$\tilde{\phi} = \arccos\left(-\frac{M_t}{2} + \frac{\sqrt{M_t^2 + 4}}{2}\right), M_t = \frac{M}{1 + \frac{1}{G^2}} \tag{2.1}$$
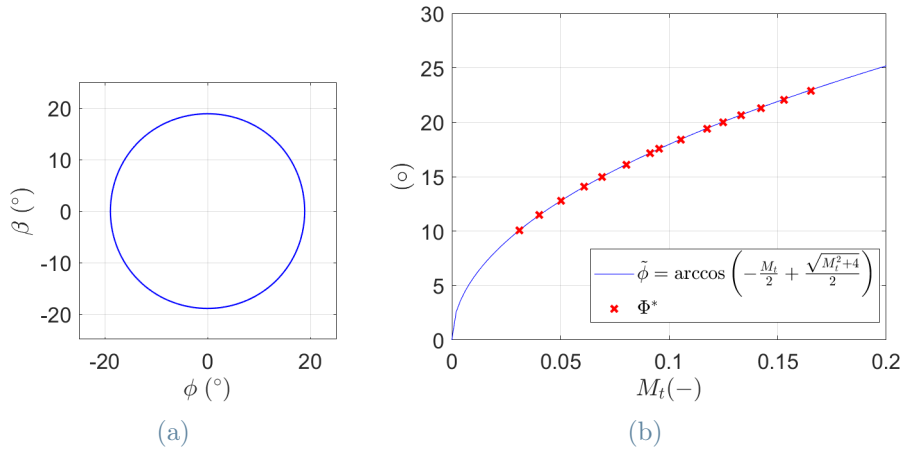

<div align="center">(a)   (b)</div>

Figure 2.2: **(a)** Represents the optimal trajectory and **(b)** optimal opening angles Φ^* (x) found by solving multiple OCPs and an analytical expression (–) as a function of the modified non-dimensional mass parameter M_t.

2.2. Optimizing for the mean mechanical power considering gravity

Now gravity has been incorporated into the modeling, and the mean mechanical power, represented as $\hat{P}_m$ (Eq. 1.25), is considered as the objective function. In the OCP, the control input ψ is modeled as a constant over time, and only one harmonic is employed for the control input γ. Furthermore, an additional equality constraint is imposed to maintain the norm of the AWES velocity $v = |\boldsymbol{v}|$ constant. To satisfy this constraint, the first Fourier coefficients of the AWES velocity ($\mathbf{R} = [V_{1,s}; V_{1,c}]$) are set to zero, as the control inputs act up to the first harmonic. No constraints are applied to the higher-order harmonics. Table 2.1 also includes the reported mean mechanical power (objective function), which is compared to the analytical formulation (Eq. 1.5) in order to evaluate their similarity.

	N_x	N_γ	N_ψ	size $\mathcal{X}$	$\mathbf{R}$	size $\mathbf{h}$	$\hat{P}_m$ (kW)	$\mathcal{T}$ (s)
OCP	10	1	0	47	$[V_{1,s}; V_{1,c}]$	44	277.21	12.65
L				analytical model			277.20	12.74

Table 2.1: Settings of the optimal control problem maximizing the mean mechanical power considering gravity. $V_{1,s}$ and $V_{1,c}$ are the first Fourier coefficients of the norm of the AWES velocity v.
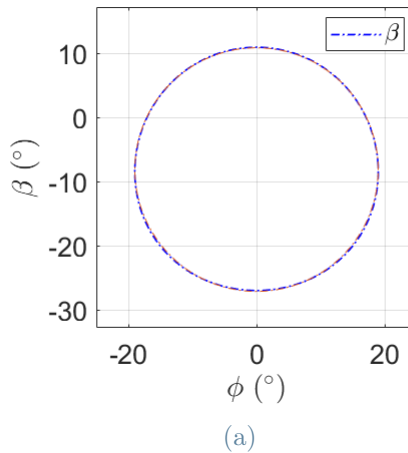

(a)

Figure 2.3: **(a)** Represents the optimal trajectory for the OCP together with a circle with radius $\tilde{\phi}$.

Upon solving the OCP, it is determined that the optimal solution exhibits a mean elevation $\hat{\beta}_B \approx$ -7.8°. The trajectory, depicted in Figure 2.3 (a), takes on a circular form although

it is not perfectly circular anymore. Furthermore, the solution of the OCP also displays a constant value of $\psi \approx 0$, indicating that the AWES span is perpendicular to the wind speed direction.
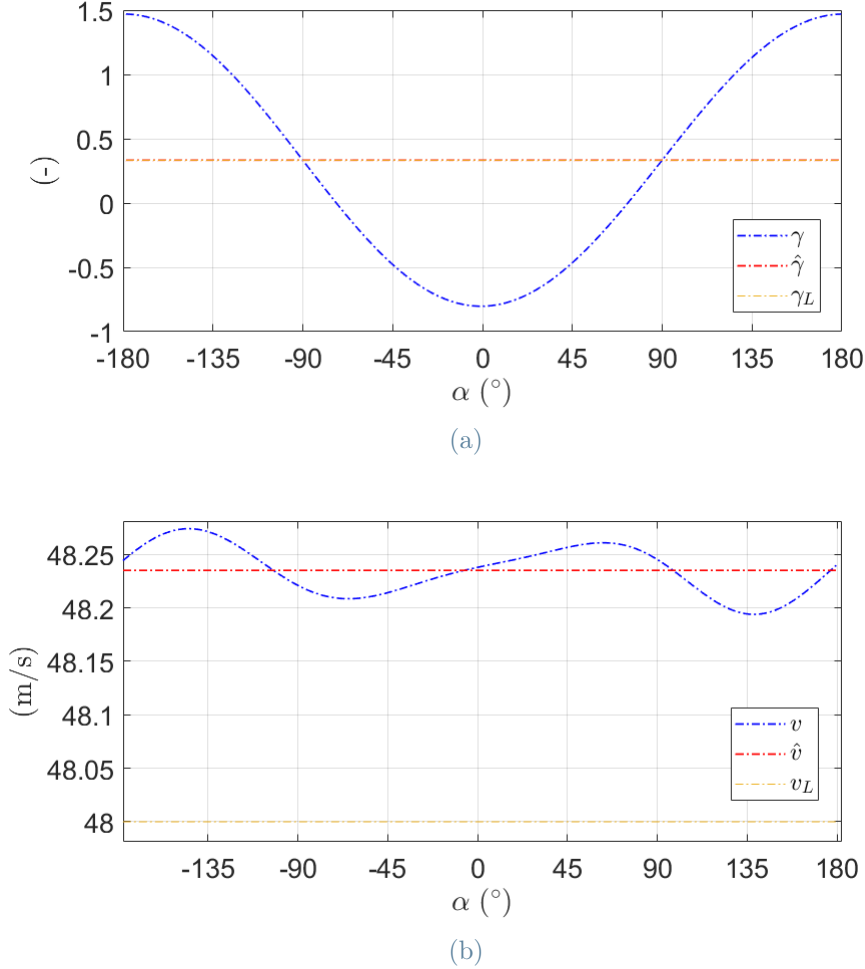

(a)

(b)

Figure 2.4: **(a)** Represents the optimal γ as a function of the angular position and **(b)** represents the norm of the optimal AWES velocity v as a function of the angular position.

Figure 2.4 (a) depicts the progression of γ as a function of α. The average value for the OCP closely aligns with the value that maximizes Eq. (1.5), indicated in the figure as γ_L. In the descending portion of the loop ($\alpha \in [90° \; \text{-}90°]$), γ attains values higher than the average, while in the ascending segment ($\alpha \in [\text{-}90° \; 90°]$), it becomes negative. This implies that during the ascending phase, there is a decrease in reel-out velocity and during the descending phase, there is otherwise an increase in this value.

Figure 2.4 (b) displays the magnitude of the optimal AWES velocity v for the OCP. This value is enforced to remain constant by imposing only the nullification of its first

harmonic. The average value of v closely aligns with the one predicted by the steady-state model therefore it is evident that the optimal trajectories are characterized by a constant AWES velocity.
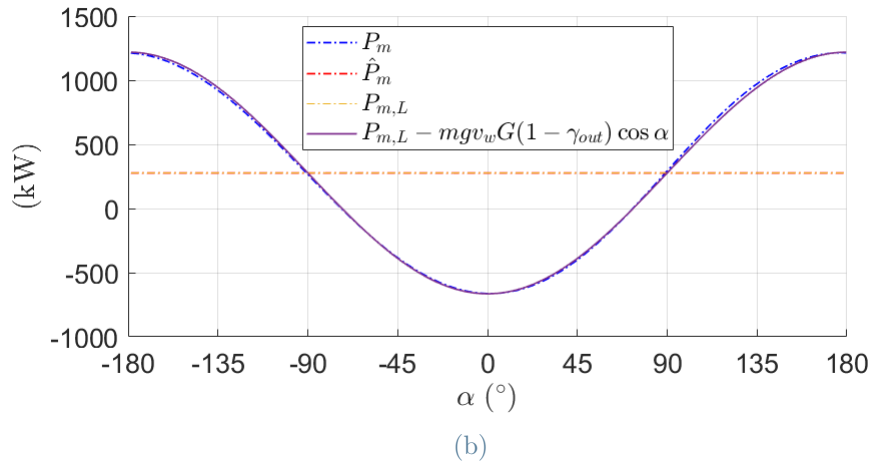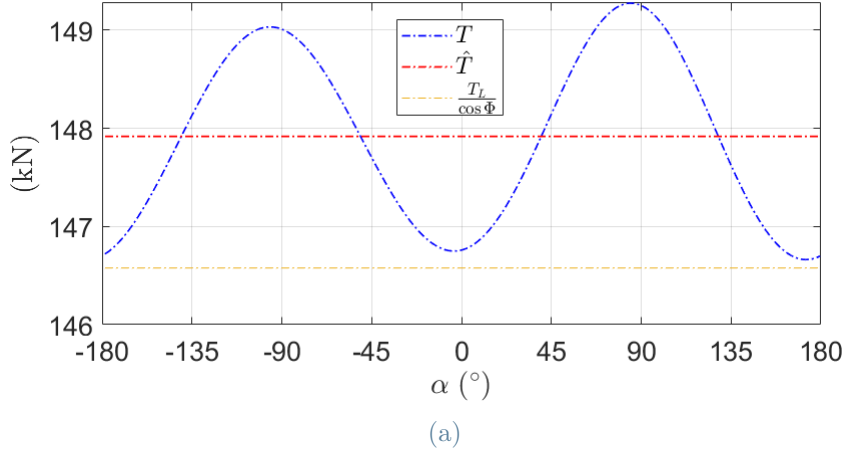

(a)

(b)

Figure 2.5: **(a)** Represents the tether force as a function of the angular position and **(b)** represents the optimal mechanical power production and consumption P_m as a function of the angular position.

Figure 2.5 (a) illustrates the magnitude of the tether force. Since the tether force is proportional to the square of the relative wind speed, it exhibits an almost constant trend (with small fluctuations compared to the mean).

In order to draw conclusions, the power output depicted in Fig. 2.5 (b) needs to be analyzed. Specifically, the descending leg leads to an increase in the mean mechanical power, while the opposite occurs with the ascending phase. The theoretical mechanical power, as given in Eq. (1.5), is derived without accounting for gravity. However, it

closely approximates the power output obtained through the OCP, which does consider the influence of gravity. Therefore, it can be stated that the optimal trajectories are characterized by the perpendicular alignment of the AWES span with respect to the wind ($\psi = 0$) and a constant AWES velocity. In order to keep the AWES velocity constant over the loop, the reel-out velocity balances the action of the gravitational force.

In addition, it is observed that in the descending portion of the loop ($\alpha \in [90°$ -90°]$), P_m attains values higher than the average, while in the ascending segment ($\alpha \in [-90°$ $90°]$), it becomes negative. This implies that during the descending phase, there is a harvest of potential energy and power production, but during the ascending phase, the power is given back to the system.

Based on these observations, the power trend, as depicted in Fig. 2.5 (b), can be approximated as follows:

$$P_m(\alpha) \approx P_{m,L} + \frac{\partial(mgh)}{\partial t} \approx P_{m,L} - mgv\cos\alpha$$
$$\approx P_{m,L} - mgv_wG(1 - \gamma_{out})\cos\alpha \tag{2.2}$$

Equation (2.2) approximates the mechanical power of the dynamic model by the sum of the steady-state mechanical power and the variation of potential energy with respect time. Where it is checked, that for the descending leg the contribution of the potential energy term contributes to an increase of the mechanical power, the opposite things occurs in the ascending leg. Also, the mechanical power can be approximated with $P_m = T_L v_w \gamma(t) \approx T_L v_w(\hat{\gamma} - A_{\gamma,1}\cos(\alpha))$. Where T_L is constant because the AWES velocity is found to be constant, so the only variable which changes with respect time is γ, being $\hat{\gamma}$ equal to γ_{out} of the steady-state model. Then, the amplitude of the first Fourier coefficient of γ, considering Eq. (2.2), can be approximated by

$$P_{m,L} \approx T_L v_w \hat{\gamma} \tag{2.3}$$

$$A_{\gamma,1} \approx \frac{mgG(1 - \gamma_{out})}{T_L} \approx \frac{mg}{\frac{1}{2}\rho AC_L v_w^2 G(1 - \gamma_{out})} = G_r G(1 - \gamma_{out}) \tag{2.4}$$

Figure 2.6 shows $A_{\gamma,1}$ found numerically by running the OCP. So, a comparison of its value with the analytical approximation given in Eq. 2.4 can be done, where $A_{\gamma,1} = 1.1443$ which is close to the difference of 1.46928 - $\hat{\gamma}$=1.1414. By checking this approach, it can be stated that due a constant AWES velocity, no variation of kinetic energy is produced

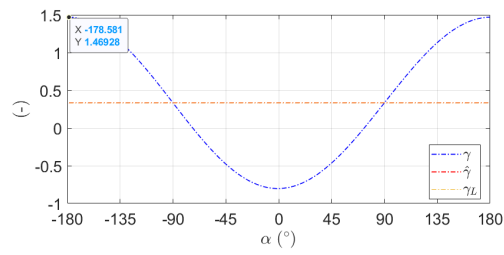over the loop, converting in this way all the potential energy into electrical.

Figure 2.6: $A_{\gamma,1}$ found numerically by running the OCP.

3 | Conclusions

This work presents a new approach for examining ideal flight paths for Ground-Gen AWES. A simplified dynamic model with two degrees of freedom is used, representing the AWES as a point mass with a fixed tether length. The degrees of freedom consist on the elevation and azimuth angles. Two control inputs are considered: the roll angle, which signifies rotation around the relative velocity direction, and γ which marks the ratio between the reel-out velocity and the wind speed. Also, the dynamic model was modified to include the reel-out velocity only in the aerodynamic terms, not it the dynamics.

To address the problem in the frequency domain, an OCP is formulated using the harmonic balance method. Using Fourier coefficients of the time series, instead of the time series themselves, offers the potential to decrease the problem's complexity, implicitly enforce periodicity, and gain a more intuitive understanding of the outcomes by analyzing the harmonic contributions.

Moreover, only the results for one OCP have been analyzed. In the OCP the control input ψ is modeled as a constant over time, and only one harmonic is employed for the control input γ. As the displayed results are pretty accurate with respect the ones of the steady-state model, there was no need in increasing the number of harmonics. Furthermore, in the work done for Fly-Gen [3] the same OCP was used and its validity checked.

Conclusions can also be obtained from the results of the optimal control problem, when considering idealized cases with uniform incoming wind speed and no constraints in the minimum elevation angle. If gravity is neglected, the solution is steady, and it can be described by analytical expressions.

If gravity is considered, the solutions are no more constant and further statements can be obtained. If the aim is to maximize the mean mechanical power considering it as the objective function, the ideal trajectories for Ground-Gen AWES are circular in shape, maintaining a constant AWES velocity and with the wing span perpendicular to the incoming wind. Also, optimal solutions present negative mean elevation angle. To achieve this optimal condition, all the potential energy is converted into electrical energy by means of a variation of reel-out velocity. This is also explained as having constant AWES velocity

means there is no kinetic energy exchange over the loop. Furthermore, the optimal power, trajectory shape, and production strategy can be effectively estimated using analytical expressions.

4 | Future developments

Regarding the future developments of this particular thesis work, more results could be done for the optimal control problem with constant inflow and no elevation angle constraints, like the optimization of the mean electrical power considering gravity. Furthermore, an optimal control problem considering gravity, wind shear and elevation angle constraint could also be studied. A validation of the frequency-domain formulation against time integration should be investigated to understand if the assumptions in the dynamic model formulation are reasonable., as similarly done for Fly-Gen [3]. Also, when defining the reel-out velocity investigating in a deeper way its link with the variation of the tether length with respect time, stating clearly the trigonometric relations between both variables.

Furthermore, the input values introduced from Makani MX2, although it is a Fly-gen AWES, they were adequate for the purpose of getting a physical understanding of the model. However, this inputs could be updated with a more suitable Ground-Gen model.

Bibliography

[1] R. Schmehl and O. Tulloch. *Airborne Wind Energy Conference 2019: (AWEC 2019)*. Glasgow, United Kingdom, 2019.

[2] Filippo Trevisi, Mac Gaunaa, and Michael Mcwilliam. Unified engineering models for the performance and cost of Ground-Gen and Fly-Gen crosswind Airborne Wind Energy Systems. *Renewable Energy*, 162:893–907, 2020.

[3] F. Trevisi, I. Castro-Fernández, G. Pasquinelli, C. E. D. Riboldi, and A. Croce. Flight trajectory optimization of fly-gen airborne wind energy systems through a harmonic balance method. *Wind Energy Science*, 7(5):2039–2058, 2022.

[4] Manuel C. R. M. Fernandes, Luís Tiago Paiva, and Fernando A. C. C. Fontes. *Optimal Path and Path-Following Control in Airborne Wind Energy Systems*, pages 409–421. Springer International Publishing, Cham, 2021.

[5] F. Trevisi, C. E. D. Riboldi, and A. Croce. Refining the airborne wind energy systems power equations with a vortex wake model. *Wind Energy Science Discussions*, 2023:1–21, 2023.

[6] N. Tucker. Airborne Wind Turbine Performance: Key Lessons From More Than a Decade of Flying Kites. In P. Echeverri, T. Fricke, G. Homsy, and N. Tucker, editors, *The Energy Kite Part I.*, pages 93–224. 2020.

[7] Grigorios Dimitriadis. *Time Integration*, chapter 3, pages 63–111. John Wiley Sons, Ltd, 2017.

List of Symbols

Variable	Description
v_w	Wind speed
L	Lift of the kite
D	Drag of the kite
R_a	Resultant aerodynamic force
T_L	Ideal tether force
v_{out}	Reel-out velocity
v_p	Perpendicular velocity to the kite
$P_{m,L}$	Ideal mechanical power of Ground-Gen
v_r	Relative velocity
α	Angle of attack of the kite
G	Glide ratio
C_L	Lift coefficient
C_D	Drag coefficient
v_h	Horizontal velocity
ρ	Air density
A	Wing area of the kite
γ_{out}	Ratio between v_{out} and v_w
AR	Aspect ratio of the kite
R_o	Radius of the trajectory of the kite
L_t	Length of the tether
P_L	Ideal electrical power of Ground-Gen
F_c	Centrifugal force of the kite
m	Mass of the kite
η_{el}	Generator and transmission efficiency

Variable	Description
M	Non dimensional mass parameter
Φ	Opening angle
$\mathcal{F}_G$	Ground reference system
$\mathcal{T}_L$	Revolution period
v_L	Norm of the AWES veclocity
F_r	Froude number
G_r	Gravity ratio
P_m	Mechanical power
P	Electrical power
$\mathbf{x}$	State vector
$\mathbf{u}$	Control vector
$\boldsymbol{N_x}$	Order of the Fourier series of the state vector
$\boldsymbol{N_u}$	Order of the Fourier series of the control vector
ω	Fundamental frequency of the motion
$\mathcal{T}$	Period of the motion
ϕ	Azimuth angle
β	Elevation angle
$\mathcal{F}_S$	AWES center of mass reference system
$\mathbf{p}$	Position of the airborne unit
$\mathbf{v}$	Velocity of the airborne unit
$\mathbf{a}$	Acceleration of the airborne unit
ψ	Roll angle
$\mathbf{s}$	Span wise unit vector
$\mathcal{X}$	Optimization variable
$\mathcal{F}_C$	Cylindrical reference frame

Acknowledgements

I would like to express my gratitude to the advisors of the thesis. Thanking Prof. Alessandro Croce for proposing me this thesis project and to Ph.D. student Filippo Trevisi for his constant support and help.